

## Early childhood stress is associated with blunted development of ventral tegmental area functional connectivity

Anne T. Park <sup>a</sup>, Ursula A. Tooley <sup>a,b</sup>, Julia A. Leonard <sup>a</sup>, Austin L. Boroshok <sup>a</sup>, Cassidy L. McDermott <sup>a</sup>, M. Dylan Tisdall <sup>c</sup>, Allyson P. Mackey <sup>a,\*</sup>

<sup>a</sup> Department of Psychology, School of Arts and Sciences, University of Pennsylvania, United States

<sup>b</sup> Neuroscience Graduate Group, Perelman School of Medicine, University of Pennsylvania, United States

<sup>c</sup> Department of Radiology, Perelman School of Medicine, University of Pennsylvania, United States

### ARTICLE INFO

**Keywords:**

Adversity  
Childhood  
Reward  
Resting-state fMRI  
Socioeconomic status

### ABSTRACT

Early life stress increases risk for later psychopathology, due in part to changes in dopaminergic brain systems that support reward processing and motivation. Work in animals has shown that early life stress has a profound impact on the ventral tegmental area (VTA), which provides dopamine to regions including nucleus accumbens (NAcc), anterior hippocampus, and medial prefrontal cortex (mPFC), with cascading effects over the course of development. However, little is known about how early stress exposure shifts the developmental trajectory of mesocorticolimbic circuitry in humans. In the current study, 88 four- to nine-year-old children participated in resting-state fMRI. Parents completed questionnaires on their children's chronic stress exposure, including socioeconomic status (SES) and adverse childhood experiences (ACEs). We found an age  $\times$  SES interaction on VTA connectivity, such that children from higher SES backgrounds showed a positive relationship between age and VTA-mPFC connectivity. Similarly, we found an age  $\times$  ACEs exposure interaction on VTA connectivity, such that children with no ACEs exposure showed a positive relationship between age and VTA-mPFC connectivity. Our findings suggest that early stress exposure relates to the blunted maturation of VTA connectivity in young children, which may lead to disrupted reward processing later in childhood and beyond.

### 1. Introduction

Early stress exposure is associated with heightened risk for poor mental health later in life (Green et al., 2010; McLaughlin et al., 2012). One mechanism by which early life stress leads to mental health vulnerability is via alterations in dopaminergic neurocircuitry (Hollon et al., 2015; Ironside et al., 2018; Russo and Nestler, 2013), which supports reward processing, cognitive flexibility, and goal-directed behavior (Lloyd and Dayan, 2016; Salamone and Correa, 2012). Disruptions to this key neural circuitry have been associated with symptoms that frequently underlie adult psychopathology, like anhedonia, impulsivity, and reduced motivation (Belujon and Grace, 2017; Novick et al., 2018). However, little is known about how stressful experiences impact dopaminergic circuitry in early childhood, a critical time point for understanding how stress causes long-term biological change.

The ventral tegmental area (VTA) in the midbrain has emerged as a key potential target for examining how stressors can have cascading effects on reward circuitry (Douma and de Kloet, 2019; Holly and

Miczek, 2016). The VTA is the primary source of dopamine projections to other reward-related regions, including the nucleus accumbens (NAcc), anterior hippocampus (aHipp), and medial prefrontal cortex (mPFC), which collectively form the mesocorticolimbic pathway (Yamaguchi et al., 2011). Recent work in rodent models has suggested that the adverse sequelae of early life stress may be critically mediated by long-lasting alterations in the VTA. Specifically, work by Peña et al. (2017) found that exposure to early life stress (during a period roughly comparable to human infancy) induced long-lasting changes in the expression of *Otx2*, a developmental transcription factor implicated in dopamine neuron development (Di Salvio et al., 2010; Omodei et al., 2008) and experience-dependent plasticity (Beurdeley et al., 2012; Lee et al., 2017), in the VTA. These mice were primed to be less resilient when they encountered additional stressors later in adulthood, i.e., they developed depression-like behavior like decreases in exploration and social approach (Peña et al., 2017). Indeed, experimentally suppressing *Otx2* in the VTA increased the likelihood of poor response to later stress, while overexpressing *Otx2* reversed the effects of early life stress,

\* Corresponding author at: 425 S. University Ave, Philadelphia, PA, 19104, United States.

E-mail address: [mackeya@upenn.edu](mailto:mackeya@upenn.edu) (A.P. Mackey).

highlighting the pivotal role of the VTA as a mediator for downstream behavior problems. Complementary work finds that stress exposure in early adolescent rats results in aberrant activity in VTA and anterior hippocampus, with evidence for a possible critical period in the vulnerability of this circuit (Gomes et al., 2019). Taken together, early life stress causes enduring alterations in the VTA that create latent vulnerability for dysregulated reward-related behaviors, perhaps via changes in the connectivity between VTA and other parts of the dopaminergic reward circuitry.

Additional work in rodents shows that VTA dopamine neurons have a protracted developmental trajectory, continuing to grow and innervate mPFC throughout adolescence (Hoops and Flores, 2017). This protracted development plays an important role in shaping the maturation of mPFC (Reynolds et al., 2018), but also leaves dopamine neurons vulnerable to environmental insult for an extended period of time. Throughout life, rodents exposed to chronic stress show loss of dopamine neurons in the VTA, and functional changes in the synaptic connections of VTA dopamine neurons to other projection targets in the mesocorticolimbic circuitry (reviewed in (Burke and Miczek, 2014; Douma and de Kloet, 2019)). Thus, chronic stress exposure has significant effects on how VTA dopamine neurons communicate with other brain regions, and may impair the mPFC's top-down regulation of the VTA. However, it is unclear how stress exposure interacts with the timing of reward circuitry development in humans.

In humans, early life stress is associated with differences in the activation and connectivity of reward processing regions, as measured by functional magnetic resonance imaging (fMRI), with the bulk of prior work focusing on the NAcc and mPFC (Hanson et al., 2016, 2017; Herzberg and Gunnar, 2020; Ironside et al., 2018). Several studies have found associations between early stress exposure and alterations in NAcc functional connectivity with medial prefrontal cortex (Fareri et al., 2017; Hanson et al., 2017; Marshall et al., 2018). For example, Hanson et al. (2017) found that childhood maltreatment was related to alterations in NAcc-mPFC task-dependent functional connectivity in young adults, but that this depended on also experiencing greater levels of recent life stress (Hanson et al., 2017), consistent with the work by Peña et al. (2017) in mice showing that early stress may sensitize the VTA to later stress. Early life stress has also been linked to reduced functional connectivity between the VTA and the hippocampus in late childhood and adolescence (Marusak et al., 2017). However, little is known about how early stress exposure impacts the developmental trajectory of VTA connectivity during childhood.

Here, we examined whether early life stress was associated with VTA resting-state functional connectivity development between the ages of 4 and 9. We additionally examined three other mesocorticolimbic regions, NAcc, aHipp, and mPFC, to test for the specificity of the effects on VTA. Resting-state is thought to reflect the history of co-activation between brain regions, making it a useful measure for probing individual differences in functional anatomy (Gabard-Durnam et al., 2016; Guerra-Carrillo et al., 2014). Its stimulus-free nature also helps mitigate the possibility that individuals from different backgrounds may differ in their familiarity with, and interpretation of, task stimuli. We conceptualized early life stress in two ways. First, we examined childhood socioeconomic status (SES). Low SES increases risk for chronic stress because it is associated with experiences like reduced access to resources, increased chaos in the home, and more exposure to violence (Evans, 2004; McLaughlin and Sheridan, 2016). Second, we examined exposure to Adverse Childhood Experiences, or ACEs, which capture children's cumulative exposure to household dysfunction, abuse, and/or neglect, in order to test whether these types of stressful home experiences uniquely explain reward circuitry differences above and beyond other negative impacts of lower SES. We investigated whether these measures of early life stress were associated with differences in the functional connectivity of VTA, NAcc, aHipp, and mPFC, and whether connectivity patterns with age differed as a function of stress exposure.

## 2. Methods

### 2.1. Participants

The Institutional Review Board at the University of Pennsylvania approved this study. All parents provided informed, written consent. Children younger than age 8 provided verbal assent, and children ages 8 and older provided written assent. Participants were recruited from Philadelphia and the surrounding regions through advertisements on public transportation, partnerships with local schools, outreach programs, community family events, and social media ads.

Resting-state scans were acquired for 137 participants. Eighty-eight participants were included in the final sample (see exclusion criteria below). Children were between the ages of 4 and 9 ( $M = 6.80$ ,  $SD = 1.38$ , range = 4.1 to 9.9). The racial and ethnic makeup of the sample was as follows: 56 % Black, 41 % White, 11 % Asian, 10 % Other, and 10 % Hispanic/Latino. Percentages sum to greater than 100 % because parents could endorse multiple races. For comparison, Philadelphia is 42.9 % Black, 35.3 % White, 6.9 % Asian, 0.5 % Other, and 12.4 % Hispanic, and the United States overall is 12.6 % Black, 62.0 % White, 5.2 % Asian, 1 % Other, and 16.9 % Hispanic (2010 US Census, StatisticalAtlas.com). We controlled for race and ethnicity in all analyses. Because the most numerous racial group was Black, we treated Black as the reference category, and included dummy variables for White, Asian, Other, and Hispanic/Latino.

Participants were excluded for: missing data on both measures of SES (parental education and income) ( $n = 1$ ), race/ethnicity ( $n = 4$ ), or the Adverse Childhood Experiences questionnaire ( $n = 8$ ); not completing the resting-state scan (e.g., due to falling asleep or wanting to end the scan early,  $n = 21$ ); an artifact in the resting-state data (due to hair glitter,  $n = 1$ ); incorrect registration of the participant at the scanner ( $n = 1$ ); or parent-reported diagnosis of Attention-Deficit/Hyperactivity Disorder during the visit, despite not reporting a diagnosis during screening ( $n = 2$ ). Participants were also excluded for having no usable resting-state data due to average head displacement (3 translations, 3 rotations) of greater than 1.2 mm ( $n = 10$ ), as well as for having an unusable structural scan ( $n = 1$ ).

### 2.2. Questionnaires

Questionnaire response distributions are shown in Fig. 1. The parent/guardian filling out the questionnaires was as follows: 80 % Mother, 17 % Father, 1 % Guardian, 2 % Grandmother. Parental education and family income were assessed using the MacArthur Foundation Research Network on Socioeconomic Status and Health sociodemographic questionnaire (Operario et al., 2004). Parents were asked to report their highest education level (possible responses ranged from "less than high school" to "professional degree (J.D., M.D., Ph.D.)"), as well as the highest education level of their partner if applicable (85 % of parents reported the education level of their partner). Average parental education ranged from 11 to 20 years ( $Mdn = 14$ ,  $SD = 2.61$ ,  $n = 88$ ). Thirty-four percent had a high school diploma or less education, compared to 58 % of adults over the age of 25 in Philadelphia, and 61.5 % in the United States (2010 US Census, StatisticalAtlas.com). Total family income was assessed by asking "Which of these categories best describes your total combined family income for the past 12 months? This should include income (before taxes) from all sources, wages, rent from properties, social security, disability and/or veteran's benefits, unemployment benefits, workman's compensation, help from relatives (including child payments and alimony), and so on." Possible responses included: Less than \$5,000, \$5,000 through \$11,999, \$12,000 through \$15,999, \$16,000 through \$24,999, \$25,000 through \$34,999, \$35,000 through \$49,999, \$50,000 through \$74,999, \$75,000 through \$99,999, \$100,000 through \$149,999, \$150,000 through \$199,999, \$200,000 and greater, and Unsure. Annual family income was estimated as the median value of the selected income bracket ( $Mdn = \$62.5$  K,  $SD =$

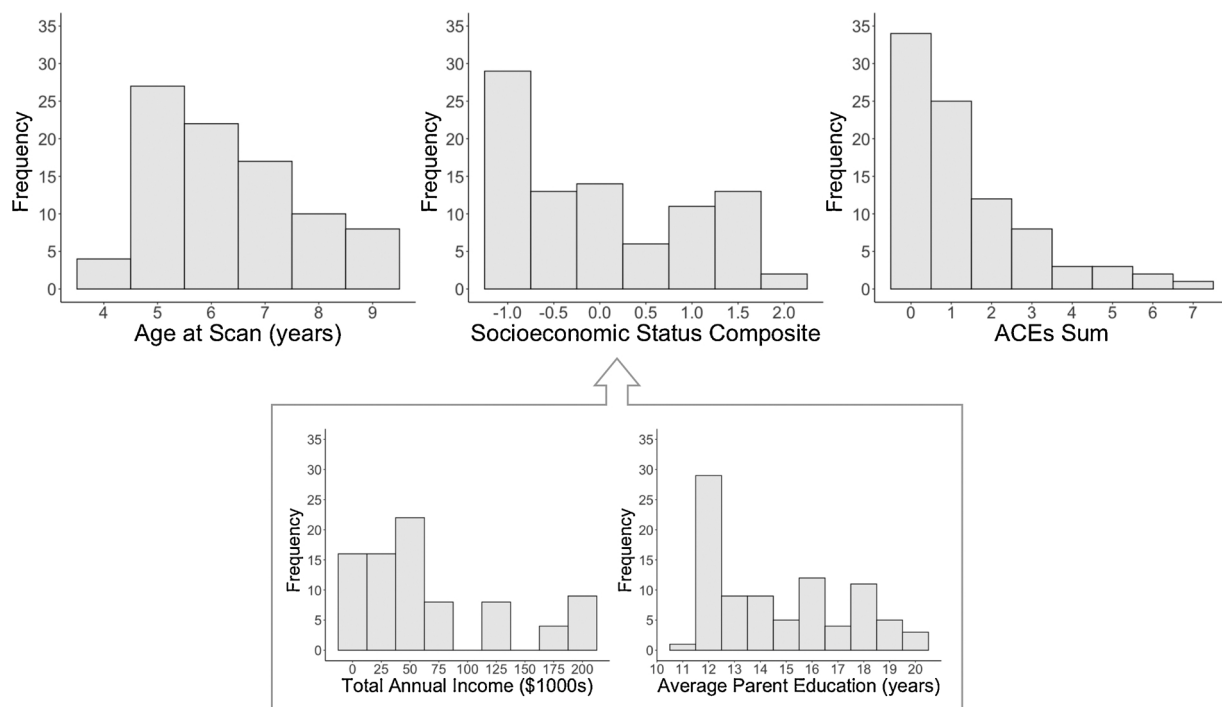


**Fig. 1.** Histograms of demographic information ( $n = 88$ ; for income,  $n = 83$ ). The Socioeconomic Status composite is the average of Z-scored income and parent education. ACEs, Adverse Childhood Experiences.

\$63 K,  $n = 83$ ). For comparison, the median household income in Philadelphia in 2010 was \$64 K, and in the United States was \$55 K. Socioeconomic status (SES) was defined as the average of Z-scored income and Z-scored years of parental education (parental education was averaged across parents if available for both parents).

Parents completed the child version of the Adverse Childhood Experiences (ACEs) questionnaire (Murphy et al., 2016), which asked parents about their child's lifetime experiences with broader household dysfunction and parent separation, abuse, and neglect. An ACEs score was calculated by summing the binary ratings for these ten types of experiences (Table 1). ACEs sum ranged from 0 to 7 ( $Mdn = 1$ ,  $SD = 1.62$ ). Number of ACEs was as follows: 38.6 % reported that their child experienced 0 ACEs, 28.4 % reported 1 ACE, and 33.9 % reported

2+ ACEs. For comparison, a nationally representative survey (2011–2014) of youth under the age of 18, using a similar ACEs measure, found that 38.5 % reported 0 ACEs, 23.5 % reported 1 ACE, and 38 % reported 2+ ACEs (Merrick et al., 2018).

### 2.3. Neuroimaging data acquisition

Prior to the scanning session, participants were acclimated to the scanning environment with a mock scanner that simulates typical MRI noises. Participants practiced keeping still in the mock scanner for about 10 min, by watching a movie that would pause each time they moved their heads more than 1 mm. During the actual MRI session, a researcher stayed in the scanner room with the participant to reassure the child and to gently squeeze the child's foot if the child moved.

Imaging was performed at the Center for Advanced Magnetic Resonance Imaging and Spectroscopy (CAMRIS) at the University of Pennsylvania. Scanning was conducted using a Siemens MAGNETOM Prisma 3 T MRI scanner with the vendor's 32-channel coil. A whole-brain, high-resolution, T1-weighted 3D-encoded multi-echo structural scan (MPRAGE) was collected (acquisition parameters: TR = 2530 ms, TEs = 1.69 ms/3.55 ms/5.41 ms/7.27 ms, BW = 650 Hz/px, 3x GRAPPA, flip angle = 7°, voxel size = 1 mm isotropic, matrix size = 256 × 256, 176 sagittal slices, FOV = 256 mm, total scan time = 4:38). This sequence used interleaved volumetric navigators to prospectively track and correct for subject head motion (Tisdall et al., 2012). A T2\*-weighted multiband gradient echo resting-state scan was also collected (acquisition parameters: multiband acceleration factor = 3, TR = 2000 ms, TE = 30.2 ms, BW = 1860 Hz/px, flip angle = 90°, voxel size = 2 mm isotropic, matrix size = 96 × 96, 75 axial slices, FOV = 192 mm, volumes = 150–240, 5 dummy scans). The multiband acceleration factor was set at 3 to balance the need for smaller voxels to localize VTA, achievable only with some acceleration, with the need for higher signal-to-noise ratios, which is reduced by higher acceleration factors, and lower motion sensitivity, which is enhanced by higher acceleration factors (Preibisch et al., 2015). Participants saw a black fixation cross on a gray screen throughout the scan.

We updated our acquisition strategy in order to increase the amount

**Table 1**

Associations between specific Adverse Childhood Experiences (ACEs) and Socioeconomic Status (SES). SES was compared between families who endorsed each item and those who did not. Negative *t*-statistics indicate lower SES for families that endorsed an item as compared to those that did not. Dashed lines indicate ACEs with too few instances to test for SES differences.

	Percentage endorsing	<i>t</i>	<i>p</i>
Parental separation/divorce	31 %	−4.69	<.001 ***
Lived with a person who ever went to prison	24 %	−8.08	<.001 ***
Lived with a person who has abused substances	24 %	−3.35	.002 **
Lived with a person who has a mental illness	23 %	−1.71	.10
Witnessed interpersonal violence	20 %	−0.39	.70
Physical neglect	9 %	1.02	.34
Emotional abuse	5 %	−1.12	.33
Emotional neglect	1 %	—	—
Sexual abuse	1 %	—	—
Physical abuse	0 %	—	—

\**p* < .05.

\*\* *p* < .01.

\*\*\* *p* < .001.

of usable data, in two ways: 1) monitoring head motion in real-time using the Framewise Integrated Real-time MRI Monitor (FIRMM) software (Dosenbach et al., 2017), and 2) collecting two resting-state scans when possible. This resulted in 54 participants who continued to be scanned until our movement criterion was achieved (at least 5 min of functional data with head motion less than 1 mm, maximum 8 min, per resting-state scan). Runs were dropped from subsequent analyses if they exceeded 1.2 mm average motion (see Summary of motion considerations), resulting in a final breakdown of 51 participants with one usable resting-state scan and 37 participants with two usable resting-state scans. All analyses controlled for the total amount of data collected (total number of resting-state volumes), as well as average motion, weighted by run length. We controlled for the amount of data provided by each child so that children with more available data would not be overrepresented in the models. Participants had an average head displacement of 0.37 mm ( $SD = 0.28$  mm, significantly non-normally distributed,  $W = 0.86$ ,  $p < .001$ ).

#### 2.4. Preprocessing

The functional imaging data were preprocessed using Nipype, a Python-based framework for flexibly integrating neuroimaging analysis tools (Gorgolewski et al., 2011). The software packages used in this preprocessing pipeline included FMRIB Software Library (FSL v5.0.8; Jenkinson et al., 2012), FreeSurfer (v6.0.0; Dale et al., 1999), Advanced Normalization Tools (ANTs v2.1.0; Avants et al., 2011)), and Nipype's implementation of Artifact Detection Tools (ART; [http://www.nitrc.org/projects/artifact\\_detect/](http://www.nitrc.org/projects/artifact_detect/)).

Simultaneous realignment and slice timing correction was conducted using an algorithm implemented in Nipy (Roche, 2011). Outlier volumes in the functional data were defined using ART based on composite motion (greater than 1 mm of head displacement between volumes) and global signal intensity (greater than 3 standard deviations from the mean).

The following confounds were regressed out of the functional data: 6 realignment parameters (3 translations, 3 rotations) and their first-order derivatives, outlier volumes flagged by ART (one nuisance regressor per outlier), composite motion, and linear and quadratic polynomials to detrend the data. Five principal components were also derived from segmentations of both cerebrospinal fluid (CSF) and white matter (WM), and regressed from the data, to correct for physiological noise like heart rate and respiration (aCompCor; Behzadi et al., 2007). The CSF and WM segmentations were derived from Freesurfer's individual parcellations of the lateral ventricles and total white matter, respectively; these segmentations were transformed into functional space. Confound regression occurred within a skull-stripped functional mask which was created using FSL's Brain Extraction Tool (BET; Smith, 2002); BET's fractional intensity threshold was set at 0.4.

The functional data were bandpass filtered (0.01–0.1 Hz), spatially smoothed with an isotropic 6 mm Gaussian kernel (FWHM), and normalized to the OASIS-30 Atropos template (in MNI152 2 mm space) in a two-step process. First, the median functional image was coregistered to the reconstructed surfaces using FreeSurfer's bbregister (Greve and Fischl, 2009); next, the structural image was registered to the OASIS-30 Atropos MNI152 template using ANTs. The transformation matrices generated by these two steps were concatenated, allowing images to be transformed directly from functional to MNI space in a single interpolation step.

#### 2.5. Seed-based analyses

We examined the functional connectivity of the ventral tegmental area (VTA), nucleus accumbens (NAcc), anterior hippocampus (aHipp), and medial prefrontal cortex (mPFC) (seeds shown in Fig. 2A). The VTA was defined using a probabilistic atlas that was constructed from hand-drawn ROIs of the VTA (Murty et al., 2014). Nucleus accumbens was

defined from the Harvard-Oxford subcortical atlas provided through FSL. Anterior hippocampus was defined from a probabilistic atlas of the medial temporal lobe (Hinday and Turk-Browne, 2016), divided into anterior and posterior sections at  $Y = -21$ , and masked by the Harvard-Oxford hippocampus in order to limit the seed from extending into surrounding white matter. Medial prefrontal cortex was defined as FreeSurfer's individual parcellation of bilateral rostral anterior cingulate cortex (rACC) based on the Desikan-Killiany atlas (Desikan et al., 2006). The seed for mPFC will be referred to throughout as rACC. The average temporal signal-to-noise ratio (tSNR) within the seed regions were as follows: VTA ( $M = 24.02$ ,  $SD = 4.39$ ), NAcc ( $M = 41.79$ ,  $SD = 9.05$ ), aHipp ( $M = 33.26$ ,  $SD = 5.10$ ), rACC ( $M = 48.65$ ,  $SD = 13.43$ ) (whole-brain tSNR maps are provided in Supplemental Fig. 1). We extracted the average time series within each ROI from unsmoothed data, to ensure that signal was not blurred outside of the ROI.

We used the average time series within each seed to generate whole-brain subject-level functional connectivity maps for the VTA, NAcc, aHipp, and rACC, using FSL's *fsLglm* tool. Because motion and physiological noise were already filtered out of the functional data during earlier preprocessing steps, subject-level GLMs only contained the seed time series as a regressor. For participants with two resting-state runs, seed connectivity maps were generated separately for each run, and then the runs were averaged together using a Nipype implementation of a fixed-effects model (using FSL's *flameo*) to produce a single connectivity map per participant to be entered into group-level analyses.

Whole-brain group-level analyses were performed with FMRIB's Local Analysis of Mixed Effects tool (FSL's FLAME 1). Only voxels that had unanimous coverage across subjects were tested, resulting in a mask that covered the entire brain. We ran the following GLMs (testing for both positive and negative associations): 1) group average; 2) main effects of age, 3) SES, and 4) ACEs exposure; and the 5) age x SES interaction and 6) age x ACEs interaction. All group GLMs included the following covariates: age (except when age was the main effect being tested), gender, average head motion (in millimeters), number of resting-state volumes, and race/ethnicity. To examine the robustness of the results, we additionally ran GLMs for SES and the age x SES interaction (GLMs 3 and 5) that controlled for the main effect of ACEs exposure, and GLMs for ACEs exposure and the age X ACEs interaction (GLMs 4 and 6) that controlled for the main effect of SES. We did not include both age x SES and age x ACEs in the same model because the regressors were collinear.

Z-statistic maps were corrected for multiple comparisons with parametric clusterwise inference using FSL's *cluster* tool (relies on Gaussian Random Field Theory) at a cluster-defining threshold of  $z = 3.1$  ( $p < .001$ ), neighborhood size of 26, and an FWE-corrected threshold of  $p < .05$ , based on evidence from Eklund et al. that false positives are not well controlled at a less stringent threshold (Eklund et al., 2016). Following recommendations for neuroimaging reporting (Poldrack, 2017), uncorrected statistical maps are available on NeuroVault (<https://neurovault.org/collections/ZSVLTSNF/>) (Gorgolewski et al., 2016). All statistical analyses were conducted in R.

#### 2.6. Summary of motion considerations

Studying brain development in early childhood requires addressing higher levels of motion than typically seen at later ages. The effect of motion during our structural scans was minimized using prospective motion correction, which provided high-quality data for our structural processing (Tisdall et al., 2012). We dealt with motion during our fMRI scans in four ways, each designed to mitigate the specific effects of motion on fMRI studies. First, we implemented real-time motion monitoring at the scanner (FIRMM) in order to more systematically track participants' motion during the scans and maximize the amount of data that met our motion thresholds (Dosenbach et al., 2017). Second, we set a motion exclusion threshold based on our data quality, as data quality differs by features of the acquisition, and therefore there is no

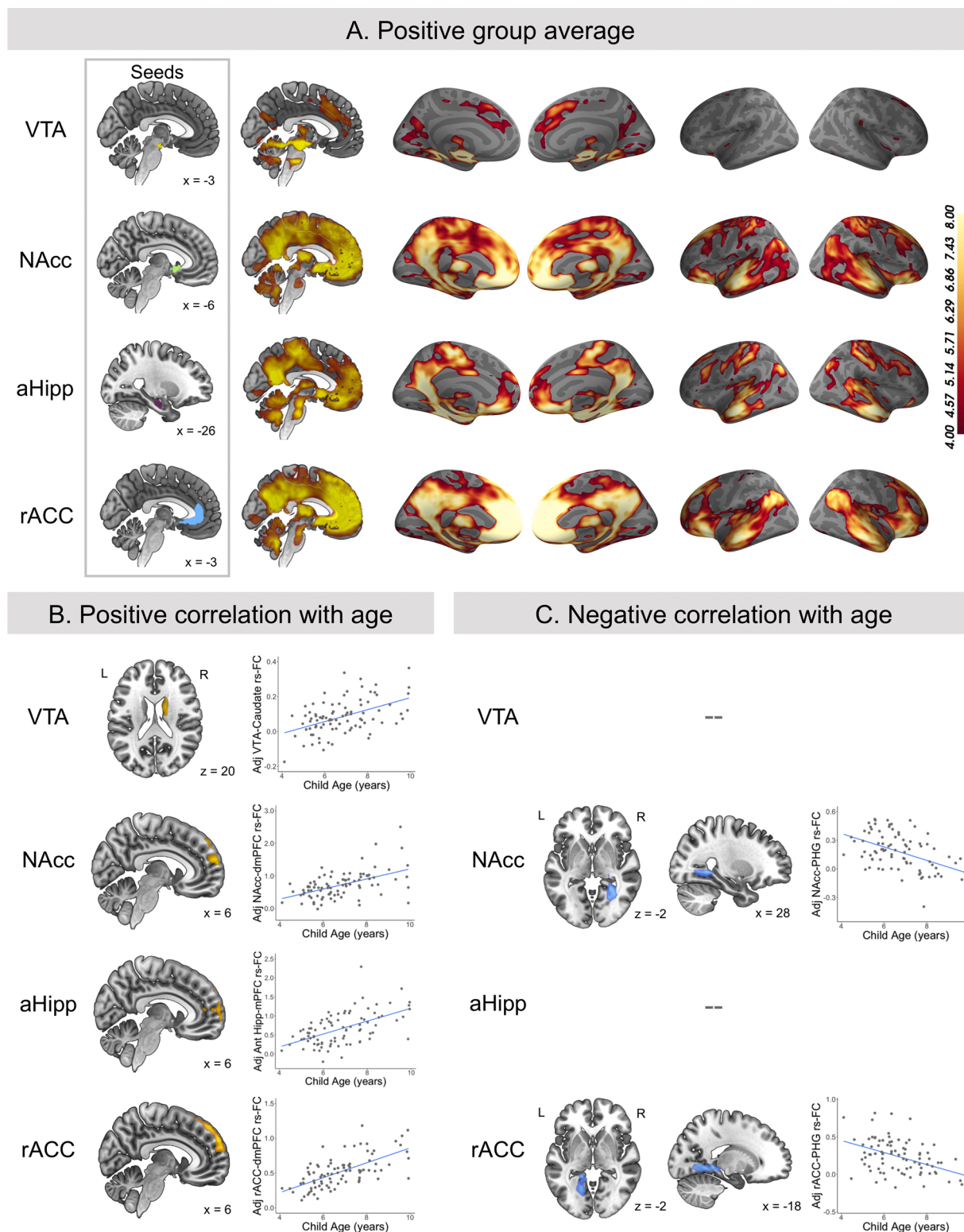


**Fig. 2.** (A) Positive group average functional connectivity for the ventral tegmental area (VTA), nucleus accumbens (NAcc), anterior hippocampus (aHipp), and rostral anterior cingulate cortex (rACC). Seed regions are shown on the left (VTA = yellow, NAcc = green, aHipp = purple, rACC = blue). (B) Positive relationships between age and functional connectivity. (C) Negative relationships between age and functional connectivity. No regions showed negative relationships between age and VTA functional connectivity, or between age and aHipp functional connectivity. Models control for age (in the group average), gender, average head motion, number of resting-state volumes, and race/ethnicity, and are corrected for multiple comparisons at  $z = 3.1$ ,  $p < 0.05$ ,  $N = 88$ . Scatterplots show the relationship between age and extracted parameter estimates (adjusted for covariates) (For interpretation of the references to color in this figure legend, the reader is referred to the web version of this article.).

universal motion cutoff that balances participant inclusion with data quality (i.e., multiband factor, head coil selection). The motion threshold was set at 1.2 mm based on qualitative evaluations of connectivity maps of a left motor cortex seed, as the anatomy of motor cortex is well-known and established by early childhood (Gao et al., 2015; Grayson and Fair, 2017). Participants with connectivity maps that did not look as expected all had composite motion over 1.2 mm. Evaluations were done by an experimenter blind to any demographic information about the participants. For participants with two usable resting-state runs, head motion was averaged between the two runs, weighted by run length. The participants who were excluded for motion ( $n = 10$ ) were slightly younger than included participants (Exc. median: 5.5 years, Inc. median: 6.6 years,  $U = 277.0$ ,  $p = .06$ ). Excluded participants did not differ from included participants on parental education (Exc. median: 15.5, Inc. median: 14,  $U = 483.0$ ,  $p = .61$ ), family income (Exc. median: \$42.5K, Inc. median: \$62.5K,  $U = 444.5$ ,  $p = .35$ ), or ACEs (Exc. median: 1, Inc. median: 1,  $U = 399.5$ ,  $p = .62$ ). Third, within the included sample, we tested how motion was related to our variables of interest: age, SES, and ACEs. Higher average head motion was significantly related to younger age ( $r_s = -0.31$ ,  $p = .003$ ) and to lower SES ( $r_s = -0.23$ ,  $p = .03$ ), but there was no age x SES interaction on head motion ( $t(84) = -0.11$ ,  $p = .91$ ). Average head motion was not significantly related to ACEs sum ( $r_s = -0.12$ ,  $p = .23$ ), and there was no age x ACEs interaction on head motion ( $t(84) = -1.06$ ,  $p = .29$ ). Fourth, because motion was related to age and SES, we included average motion (across runs) in all models.

### 3. Results

#### 3.1. Demographics and stress measures

Lower SES was associated with greater exposure to ACEs ( $r_s = -0.32$ ,  $p = .002$ ). Specifically, SES was lower among children who experienced parental separation ( $t(86) = -4.69$ ,  $p < .001$ ), family incarceration ( $t(86) = -8.08$ ,  $p < .001$ ), and family drug abuse ( $t(86) = -3.35$ ,  $p = .002$ ) (Table 1). ACEs exposure was lower for White children than for Black children ( $t(83) = -2.63$ ,  $p = .01$ ). SES was higher for White ( $t(83) = 4.74$ ,  $p < .001$ ) and Asian ( $t(83) = 4.75$ ,  $p < .001$ ) children than for Black children. ACEs exposure was slightly, but not significantly, higher in Hispanic children as compared to Non-Hispanic children ( $t(83) = 1.43$ ,  $p = .16$ ). SES was slightly, but not significantly, lower in Hispanic children as compared to Non-Hispanic children ( $t(83) = -1.77$ ,  $p = .08$ ). Age was not significantly related to SES ( $r_s = -.17$ ,  $p = .12$ ), but it was significantly positively related to ACEs ( $r_s = 0.26$ ,  $p = .01$ ). SES and ACEs exposure did not differ by gender.

#### 3.2. Group average results

Across the entire group, VTA was positively functionally connected to subcortical regions including nucleus accumbens, hippocampus, amygdala, and cerebellum, as well as the striatum and thalamus (Fig. 2A). In cortex, VTA was most strongly correlated with medial prefrontal cortex, precuneus, and visual cortex, broadly consistent with D<sub>1</sub> receptor binding sites in the human brain (Palomero-Gallagher et al., 2015). Notably, we did not observe strong connectivity with lateral prefrontal and parietal regions in this age range, consistent with developmental work on VTA connectivity (Tomasi and Volkow, 2014). The positive group averages for NAcc, aHipp, and rACC were similar, showing broad connections to subcortical regions and to the default mode network. NAcc and aHipp additionally showed connectivity with somatomotor cortex. There were no regions that showed negative functional connectivity in the group average for the VTA, NAcc, aHipp, or rACC.

#### 3.3. Main effects of age

VTA functional connectivity showed a positive association with age in the right caudate (Fig. 2B; peak voxel coordinates (MNI): 14, 2, 20, maximum z-statistic = 4.09, cluster volume = 171 voxels). No regions showed a negative age-related association with VTA functional connectivity. NAcc, rACC, and aHipp functional connectivity showed positive associations with age in dorsal medial prefrontal cortex (dmPFC) (Fig. 2B, NAcc peak voxel coordinates (MNI): 6, 62, 18, maximum z-statistic = 4.42, cluster volume = 372 voxels; aHipp peak voxel coordinates (MNI): -2, 52, 10, maximum z-statistic = 4.44, cluster volume = 475 voxels; rACC peak voxel coordinates (MNI): 8, 48, 46, maximum z-statistic = 5.38, cluster volume = 1788 voxels). aHipp functional connectivity also showed a positive association with age in two additional clusters (Fig S2): right cerebellum (peak voxel coordinates (MNI): 42, -62, -44, maximum z-statistic = 4.72, cluster volume = 349 voxels); and left dorsal PFC (peak voxel coordinates (MNI): -20, 24, 60, maximum z-statistic = 4.52, cluster volume = 521 voxels).

NAcc and rACC connectivity showed similar negative associations with age (Fig. 2C). NAcc connectivity showed a negative relationship with age in right parahippocampal gyrus (PHG; peak voxel coordinates (MNI): 28, -48, -2, maximum z-statistic = 4.43, cluster volume = 388 voxels), and rACC connectivity showed a negative relationship with age in left PHG (peak voxel coordinates (MNI): -18, -42, -2, maximum z-statistic = 4.28, cluster volume = 436 voxels). No negative relationship with age was found for aHipp.

#### 3.4. Main effects of stress measures

Higher SES was related to lower VTA functional connectivity with bilateral intraparietal sulcus (Fig. 3A; right IPS: peak voxel coordinates (MNI): 30, -54, 42, maximum z-statistic = 4.70, cluster volume = 242 voxels; left IPS: peak voxel coordinates (MNI): -22, -56, 38, maximum z-statistic = 4.50, cluster volume = 553 voxels). The main effect of SES was similar when additionally controlling for ACEs exposure, although limited only to left IPS (Fig S3A). Higher ACEs exposure was related to lower VTA functional connectivity with right somatomotor cortex (Fig. 3B; peak voxel coordinates (MNI): 64, -2, 26, maximum z-statistic = 4.55, cluster volume = 213 voxels). The main effect of ACEs exposure was highly similar when additionally controlling for SES (Fig S3B). No regions showed a positive association with VTA functional connectivity for SES or ACEs exposure. There were no significant positive or negative main effects of SES or ACEs exposure on NAcc, aHipp, or rACC functional connectivity.

#### 3.5. Interactions between age and stress measures

There was an age x SES interaction on connectivity between VTA and left dorsal mPFC (dmPFC) (Fig. 4A; peak voxel coordinates (MNI): -10, 40, 24, maximum z-statistic = 4.38, cluster volume = 509 voxels). VTA-dmPFC connectivity showed a stronger positive association with age in children from higher SES backgrounds, compared to children from lower SES backgrounds. The age x SES interaction was nearly identical after additionally controlling for the main effect of exposure to ACEs (Fig S4A). To examine whether the relationship between age and VTA connectivity is significantly different from zero within SES groups, participants were divided into 2 groups by median split: higher SES ( $n = 46$ ) and lower SES ( $n = 42$ ). VTA-dmPFC connectivity was positively related to age in children from a higher SES background ( $t(77) = 4.56$ ,  $p < .001$ , 95 % CI [0.02, 0.06]), and not significantly related to age in children from a lower SES background ( $t(77) = -1.52$ ,  $p = .13$ , 95 % CI [-0.04, 0.005]; Fig. 4A).

We found a similar age x ACEs interaction on connectivity between VTA and left dorsal mPFC (Fig. 4B; peak voxel coordinates (MNI): -14, 36, 36, maximum z-statistic = 4.43, cluster volume = 564 voxels). VTA-dmPFC connectivity showed a stronger positive association with age in

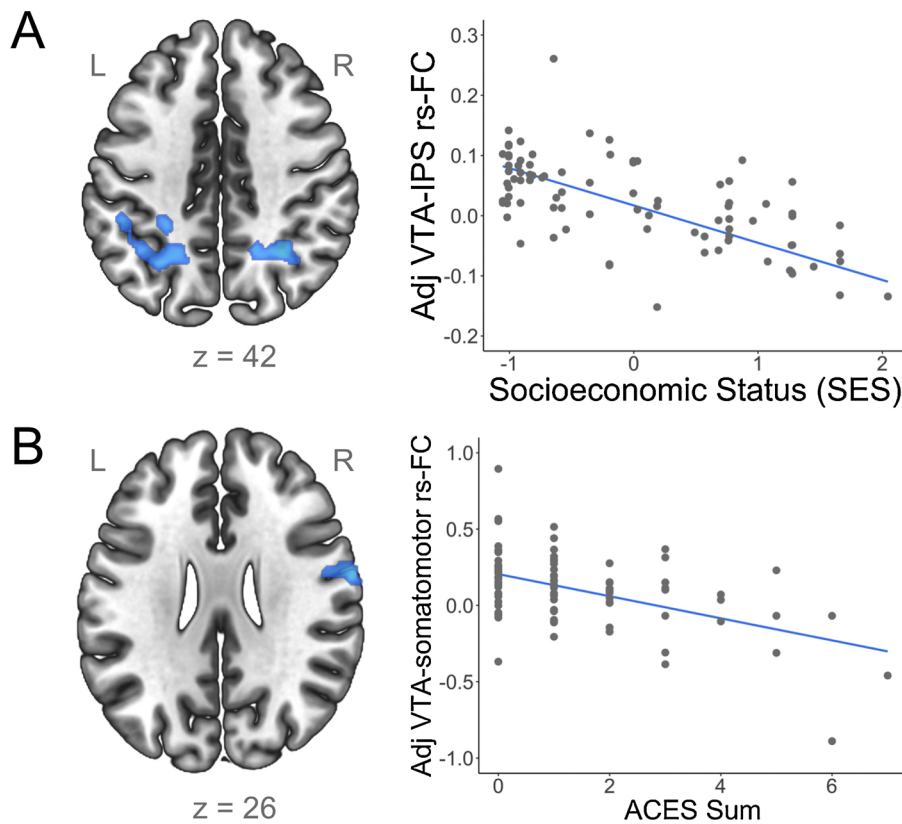


**Fig. 3.** (A) Higher Socioeconomic Status (SES) is associated with lower ventral tegmental area (VTA) functional connectivity with bilateral intraparietal sulcus (IPS). (B) Higher exposure to Adverse Childhood Experiences (ACEs) is associated with lower VTA functional connectivity with right somatomotor cortex. Models control for age, gender, average head motion, number of resting-state volumes, and race/ethnicity. Results are corrected for multiple comparisons at  $z = 3.1$ ,  $p < 0.05$ . Scatterplots show the relationship between the independent variables (SES, ACEs) and extracted parameter estimates (adjusted for covariates).

children with lower exposure to ACEs, compared to children with higher exposure to ACEs. The dmPFC cluster overlapped with the age x SES result but additionally extended to the lateral surface of PFC. The age x ACEs interaction was almost identical after additionally controlling for the main effect of SES (Fig S4B). To test whether the relationship between age and VTA connectivity is significantly different from zero within ACEs exposure levels, participants were divided into 3 groups: exposure to 0 ACEs ( $n = 34$ ), 1 ACE ( $n = 25$ ), or 2 or more ACEs ( $n = 29$ ). The 2+ ACEs group reflects greatest cumulative risk, while the 1 ACE group is heterogeneous in its experiences (32 % parental separation/divorce, 24 % living with someone with mental illness, 20 % witnessing adults treated violently, 12 % physical neglect, 4 % living with someone who abuses substances, 4 % living with someone who has been incarcerated, 4 % sexual abuse). VTA-dmPFC connectivity was positively related to age in children with no ACEs exposure ( $t(74) = 3.45$ ,  $p = .001$ , 95 % CI [0.02, 0.09]), positively related to age in children with exposure to 1 ACE ( $t(74) = 2.19$ ,  $p = .03$ , 95 % CI [0.004, 0.08]), and unrelated to age in children with 2+ ACEs ( $t(74) = -1.95$ ,  $p = .055$ , 95 % CI [-0.06, 0.0006]); Fig. 4B).

There was an age x ACEs interaction on connectivity between aHipp and left inferior frontal gyrus (IFG) (Fig. 4C; peak voxel coordinates (MNI): -40, 4, 22, maximum z-statistic = 4.23, cluster volume = 352 voxels). aHipp-LIFG connectivity showed a stronger negative association with age in children with higher exposure to ACEs, compared to children with lower exposure to ACEs. The age x ACEs interaction was nearly identical after additionally controlling for the main effect of exposure to SES (Fig S4C). aHipp-LIFG connectivity was unrelated to age in children with no ACEs exposure ( $t(74) = 0.84$ ,  $p = .40$ , 95 % CI [-0.04, 0.11]), unrelated to age in children with exposure to 1 ACE ( $t(74) = -0.35$ ,  $p = .73$ , 95 % CI [-0.10, 0.07]), and negatively related to age in children with 2+ ACEs ( $t(74) = -2.33$ ,  $p = .02$ , 95 % CI [-0.14, -0.01]); Fig. 4C). There was no significant age x SES interaction for the aHipp seed, and no significant age x SES or age x ACEs exposure interactions for the NAcc or rACC seeds.

#### 4. Discussion

Resting-state functional connectivity of the ventral tegmental area (VTA) showed different patterns with age as a function of stress exposure in 4- to 9-year-old children. Specifically, children from higher socioeconomic status (SES) backgrounds showed age-related increases in VTA functional connectivity with dorsal medial prefrontal cortex (dmPFC), while children from lower SES backgrounds did not show this pattern. Similarly, only children with low exposure to Adverse Childhood Experiences (ACEs) showed age-related increases in VTA functional connectivity with dmPFC. Our results suggest that stress-related differences in VTA connectivity begin to emerge during childhood. It is possible that children from lower SES backgrounds or with high ACEs exposure accumulate negative experiences as they grow up, or that they do not accumulate positive experiences in the same way as their peers from lower stress backgrounds. It is also possible that early experiences, before age 4, set children on different developmental trajectories. Longitudinal work beginning in infancy or even at conception, with detailed information on the specific timing of stressors, is needed to better understand the causes of the cross-sectional relationships presented here.

Our findings are consistent with recent work in rodents showing that exposure to early life stress causes changes in the VTA that create susceptibility to later stressors ((Peña et al., 2017)). There is evidence that chronic stress results in the loss of dopaminergic neurons in the VTA (Sugama and Kakinuma, 2016), as well as altered dopamine activity in VTA projection targets like NAcc and mPFC (Holly and Miczek, 2016). Stress also has been shown to alter mPFC neuron morphology (Cook and Wellman, 2004; Liston et al., 2006). Communication between VTA and mPFC is complex and bidirectional, with both excitatory and inhibitory connections determining dopamine activity (Beier et al., 2015). Studies in animal models have not yet determined whether early life stress impacts projections from VTA, or projections to VTA from mPFC. Unfortunately, resting-state fMRI cannot differentiate between excitatory and inhibitory connections, and analytical approaches that can shed light

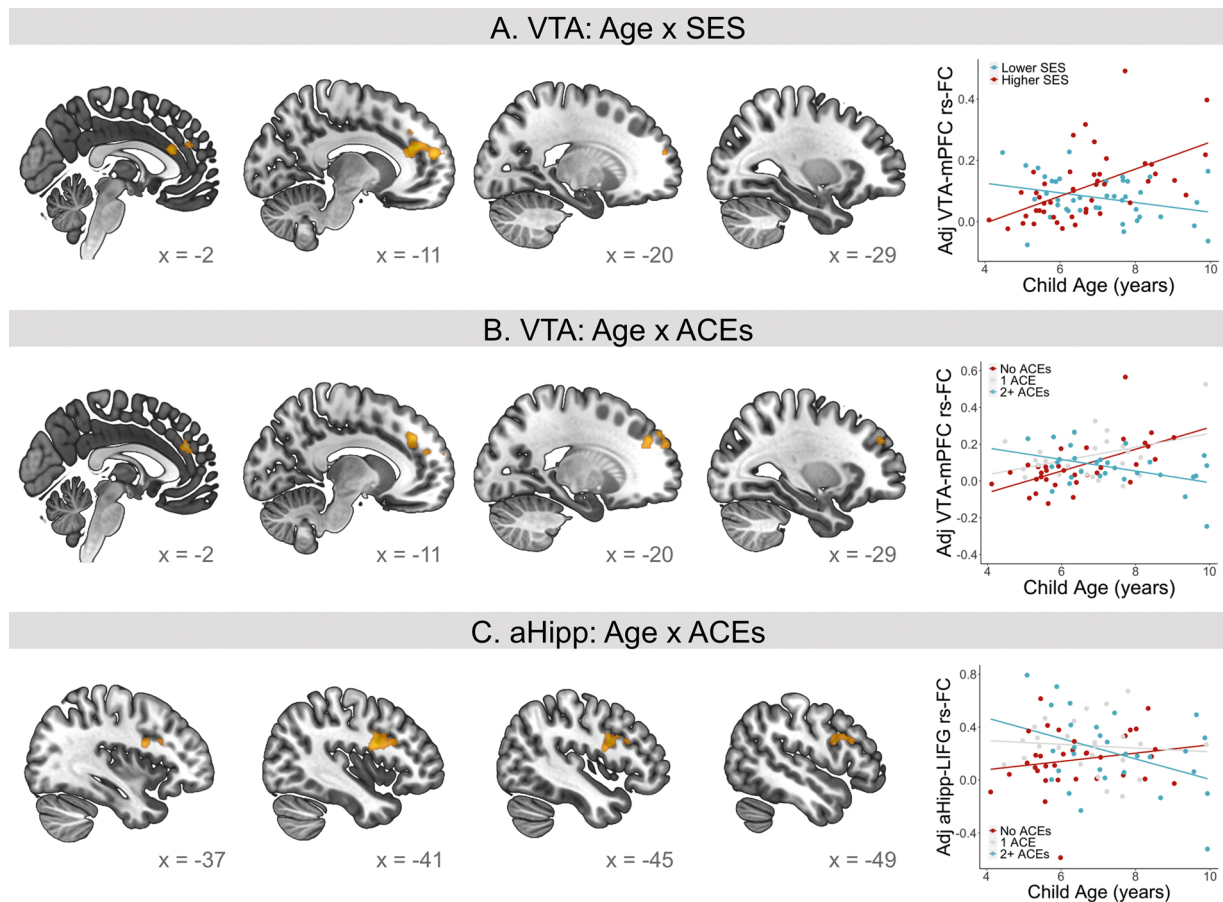


**Fig. 4.** (A) Age x Socioeconomic Status (SES) interaction on ventral tegmental area (VTA) functional connectivity. Scatterplot shows the relationship between child age and extracted parameter estimates, plotted by median split on SES for visualization purposes. (B) Age x Adverse Childhood Experiences (ACEs) interaction on VTA functional connectivity. (C) Age x ACEs interaction on anterior hippocampus (aHipp) functional connectivity. Scatterplots show the relationship between age and extracted parameter estimates (adjusted for covariates). For visualization purposes, participants were grouped by having exposure to 0, 1, or 2+ ACEs. Results are corrected for multiple comparisons at  $z = 3.1, p < 0.05$ . All models control for gender, average head motion, number of resting-state volumes, and race/ethnicity.

onto directionality, i.e., bottom-up vs. top-down, require more data than can be acquired in young children (Mitra et al., 2015). Our work is also consistent with cross-species evidence that the development of VTA projections in rodents (Hoops and Flores, 2017), and the maturation of dopamine availability in humans (Larsen et al., 2020), continues through childhood and adolescence.

The age x ACEs and age x SES interactions on VTA connectivity were observed in a region of mPFC that is often called dorsal anterior cingulate cortex (dACC). The dACC has been hypothesized to play an important role in appraising environmental states and integrating internal and external motivational factors, in order to guide behavior via top-down modulation of the VTA (Beier et al., 2015; Haber and Behrens, 2014; Heilbronner and Hayden, 2016). Blunted age-related changes in VTA-mPFC functional coupling in childhood may thus reflect alterations in effective dACC top-down regulation of dopamine activity. Recent work also suggests that the dopaminergic midbrain drives dorsal mPFC's role in learning about the amount of effort needed to perform a task, highlighting the bottom-up influences that additionally support motivated behavior (Hauser et al., 2017). We did not observe any age x stress interactions on nucleus accumbens (NAcc) or rostral anterior cingulate cortex (rACC) connectivity, but we did observe that connectivity between anterior hippocampus and left inferior frontal gyrus (LIFG) differed by ACEs exposure. aHipp-LIFG connectivity showed a stronger negative association with age in children with higher exposure to ACEs, compared to children with lower exposure to ACEs. It has been suggested that dopaminergic neuromodulation may play a critical role in refining hippocampal-prefrontal circuitry during adolescence, in

support of goal-oriented behavior and decision making (Murty et al., 2016).

Across our entire sample of children, irrespective of stress exposure, we found that the VTA showed increased connectivity with the caudate with age. This finding is consistent with prior work showing greater VTA-caudate connectivity in adults (ages 15–46) relative to youth (ages 7–22, but note overlapping age ranges) (Tomasi and Volkow, 2014). The caudate plays an important role in behaviors like performance monitoring and cognitive control (Brovelli et al., 2011). Indeed, recent work in young adults has shown that the structural connectivity between VTA and caudate is related to conflict monitoring (Mamiya et al., 2019). Thus, increased functional coupling between the VTA and caudate may support the rapid development of cognitive control between the ages of 4 and 9 (Akshoomoff et al., 2018; Fjell et al., 2012). We also found that NAcc, aHipp, and rACC show very similar positive relationships between age and connectivity with dmPFC. Past work found different developmental changes in NAcc resting-state connectivity, i.e., decreased connectivity between NAcc and subgenual ACC, but the age range was much broader, from 4 and 23 (Fareri et al., 2015). Another study found no developmental changes in VTA-NAcc connectivity at rest in adolescence and young adulthood (ages 10–30), but found that VTA-NAcc connectivity during a motivational task decreased with age (Murty et al., 2018). Reward system development is likely nonlinear through adolescence and differs by task state (Hartley and Somerville, 2015; Somerville et al., 2010; Somerville and Casey, 2010). We also observed age-related decreases in connectivity between rACC and NAcc with the parahippocampal gyrus (PHG), a region involved in spatial processing and

memory. PHG is at the border of visual and default mode networks in adults, depending on the parcellation (Yeo et al., 2011), but little is known about how its network membership changes with development. Fareri and colleagues found a positive relationship between age and NAcc-PHG connectivity in their broad age range of 4–23 (Fareri et al., 2015), suggesting that changes early in childhood may not extend linearly through adolescence and early adulthood.

We observed a negative main effect of SES on VTA connectivity with bilateral intraparietal sulcus (IPS), a task-positive region spanning the frontoparietal network (FPN) and the dorsal attention network (DAN; Yeo et al., 2011), and implicated in processing number and space (Hubbard et al., 2005). Parietal cortex more broadly is rich in dopamine receptor expression (Palomero-Gallagher et al., 2015), but few parietal neurons project back down to VTA (Watabe-Uchida et al., 2012), suggesting that our result reflects differences in bottom-up innervation of IPS by VTA neurons. The cognitive implications of lower VTA-IPS connectivity are unclear. We additionally observed a main effect of ACEs exposure on VTA connectivity, such that higher ACEs exposure was associated with lower connectivity between VTA and right ventral somatomotor cortex, a region that does directly project to VTA (Watabe-Uchida et al., 2012), and has been linked to action-related learning (Coddington and Dudman, 2019). Further research is needed to replicate this unexpected finding and determine the behavioral relevance of adversity effects on VTA-somatomotor connectivity. In contrast with prior studies in older children (Marusak et al., 2017; Richter et al., 2019), we did not observe a main effect of stress on hippocampal connectivity, nor did we find stress effects on connectivity of NAcc or rACC.

SES and ACEs exposure were moderately correlated at about .3. The main effects of ACEs and SES on VTA connectivity were distinct, and held even when controlling for the other stress measure. The interactions between stress measures and age were highly similar, suggesting that both measures have similar effects on the maturation of VTA connectivity with mPFC. It will be critical in future work to examine how a broader set of stressors have unique impacts on the early organization of dopaminergic circuitry (Palacios-Barrios and Hanson, 2019). This would include experiences such as negative parenting behaviors, lack of social support, a chaotic and/or dangerous home environment, broader community disadvantage, and racial discrimination. In this study, as in many others, race was associated with SES and ACEs exposure. We controlled for race, rather than examine its impacts directly, because our samples within racial groups were small, and because we did not collect data on individuals' experiences with racism, which likely constitute major stressors for families of color.

This study has a number of limitations. First, our data are cross-sectional, so although we have demonstrated a possible age-related blunting of reward circuitry development, we have not yet followed children as they grow up. Second, our measures of early stress exposure rely on parents accurately and completely reporting on their children's experiences. It is possible that some parents under-report on child ACEs due to a lack of complete knowledge about their child's experiences, poor memory for retrospective events, or the sensitive nature of some of the items (e.g., abuse and neglect). Our definition of SES, which combines parent education and income, is also limited since it is a snapshot measure that may not capture potentially important household dynamics, like changes in partner or changes in income. Future work should also examine whether similar findings are found in population representative samples. Third, our measures of SES and ACEs exposure reflect cumulative and chronic stressors, and thus we cannot draw conclusions about the nature of the stressors impacting VTA connectivity. Future work could take a more dimensional approach, to see if particular types of stressors are driving these effects (McLaughlin and Sheridan, 2016), and to explore what other environmental experiences associated with lower SES are impacting VTA-mPFC connectivity in early childhood. It will also be important to further investigate the timing of adversity, i.e., whether alterations in VTA connectivity emerge due to the cumulative impact of stressors encountered over time, or due

to the pivotal impact of a stressor experienced during an early sensitive window. Fourth, it is possible that certain VTA connectivity relationships may only emerge during task-dependent states (Ballard et al., 2011; Murty et al., 2018; Salehi et al., 2020). Future work should examine developmental patterns in VTA connectivity during motivational contexts. Fifth, we are limited by the spatial resolution of our fMRI data, as the VTA is a small brain region flanked closely by the substantia nigra (part of the nigrostriatal dopamine pathway). Thus, it is possible that some of our findings reflect connectivity of the midbrain more broadly rather than VTA alone. We also note that the signal-to-noise ratio (SNR) in VTA was lower than that of the other seed regions. Fifth, resting-state connectivity relies on blood oxygen-level dependent (BOLD) signal and therefore can be influenced by individual differences in vasculature and physiology (K. Murphy et al., 2013; Shmueli et al., 2007), though these relationships may be functionally important and not just confounds (Tak et al., 2015). Cardiovascular function is impacted by SES and ACEs in adolescents and adults (Lagraauw et al., 2015; Low et al., 2009; Monnat and Chandler, 2015), but the links are less well-studied in children, and it is unclear how physiological differences would result in the specific pattern of findings presented here.

In sum, our findings suggest that early stress exposure may disrupt the typical developmental trajectory of the dopamine system, which is essential for reward processing and goal-directed behavior. Future work should examine how early life stress impacts the interplay between VTA, a broader set of subcortical regions, and cortical networks, as well as its consequences for a variety of behaviors, like impulse control (Zisner and Beauchaine, 2015), effortful behavior (Assadi et al., 2009; Westbrook et al., 2020), exploration (Laureiro-Martínez et al., 2015), and curiosity (Gruber and Ranganath, 2019). We hypothesize that a blunted VTA-mPFC developmental trajectory could serve as a biomarker for reduced resilience to stress: these children may be more at risk for the development of psychopathology following stressors experienced later in life. In order to help buffer against the long-lasting and potentially compounding effects of early disruptions to reward neurocircuitry, it will be critical to design early childhood interventions that help children develop effective strategies for coping with chronic stress, and that focus on positive development of motivated behavior.

#### Declaration of Competing Interest

The authors report no declarations of interest.

#### Acknowledgments

We would like to first thank all of the families who participated in this research. We would like to thank Jasmine Forde, Katrina Simon, Sophie Sharp, Yoojin Hahn, Stephanie Bugden, Jamie Bogert, Alexis Broussard, Ava Cruz, Samantha Ferleger, Destiny Frazier, Jessica George, Abigail Katz, Sun Min Kim, Hunter Liu, Dominique Martinez, Ortal Nakash, Emily Orengo, Christina Recto, Leah Sorcher, and Alexis Uria for their help with data acquisition. Finally, we would like to thank Catherine Jensen Peña for guidance on the study's hypotheses and feedback on initial results. This study was supported by the Jacobs Foundation Early Career Award (A.P.M.), NIDA (1R34DA050297-01 to M.D.T. and A.P.M.), Behavioral and Cognitive Neuroscience Training Grant (NIH T32-MH017168 to A.T.P.), the MindCORE postdoctoral research fellowship from the University of Pennsylvania to J.A.L., and National Science Foundation Graduate Research Fellowships to U.A.T., A.L.B., and C.L.M under Grant No. DGE-1845298.

#### Appendix A. Supplementary data

Supplementary material related to this article can be found, in the online version, at doi:<https://doi.org/10.1016/j.dcn.2020.100909>.

## References

- Akshoomoff, N., Brown, T.T., Bakeman, R., Hagler, D.J., 2018. Developmental differentiation of executive functions on the NIH Toolbox Cognition Battery. *Neuropsychology* 32 (7), 777–783. <https://doi.org/10.1037/neu0000476>.
- Assadi, S.M., Yücel, M., Pantelis, C., 2009. Dopamine modulates neural networks involved in effort-based decision-making. *Neurosci. Biobehav. Rev.* 33 (3), 383–393. <https://doi.org/10.1016/j.neubiorev.2008.10.010>.
- Avants, B.B., Tustison, N.J., Song, G., Cook, P.A., Klein, A., Gee, J.C., 2011. A reproducible evaluation of ANTS similarity metric performance in brain image registration. *NeuroImage* 54 (3), 2033–2044. <https://doi.org/10.1016/j.neuroimage.2010.09.025>.
- Ballard, I.C., Murty, V.P., Carter, R.M., MacInnes, J.J., Huettel, S.A., Adcock, R.A., 2011. Dorsolateral prefrontal cortex drives mesolimbic dopaminergic regions to initiate motivated behavior. *The Journal of Neuroscience: The Official Journal of the Society for Neuroscience* 31 (28), 10340–10346. <https://doi.org/10.1523/JNEUROSCI.0895-11.2011>.
- Behzadi, Y., Restom, K., Liau, J., Liu, T.T., 2007. A component based noise correction method (CompCor) for BOLD and perfusion based fMRI. *NeuroImage* 37 (1), 90–101. <https://doi.org/10.1016/j.neuroimage.2007.04.042>.
- Beier, K.T., Steinberg, E.E., DeLoach, K.E., Xie, S., Miyamichi, K., Schwarz, L., Gao, X.J., Kremer, E.J., Malenka, R.C., Luo, L., 2015. Circuit architecture of VTA dopamine neurons revealed by systematic input-output mapping. *Cell* 162 (3), 622–634. <https://doi.org/10.1016/j.cell.2015.07.015>.
- Belluon, P., Grace, A.A., 2017. Dopamine system dysregulation in major depressive disorders. *The International Journal of Neuropsychopharmacology / Official Scientific Journal of the Collegium Internationale Neuropsychopharmacologicum* 20 (12), 1036–1046. <https://doi.org/10.1093/ijnp/pyx056>.
- Beurdeley, M., Spatazza, J., Lee, H.H.C., Sugiyama, S., Bernard, C., Di Nardo, A.A., Hensch, T.K., Prochiantz, A., 2012. Otx2 binding to perineuronal nets persistently regulates plasticity in the visual cortex. *J. Neurosci.* 32 (27), 9429–9437. <https://doi.org/10.1523/JNEUROSCI.0394-12.2012>.
- Brovelli, A., Nazarian, B., Meunier, M., Boussaoud, D., 2011. Differential roles of caudate nucleus and putamen during instrumental learning. *NeuroImage* 57 (4), 1580–1590. <https://doi.org/10.1016/j.neuroimage.2011.05.059>.
- Burke, A.R., Miczek, K.A., 2014. Stress in adolescence and drugs of abuse in rodent models: role of dopamine, CRF, and HPA axis. *Psychopharmacology* 231 (8), 1557–1580. <https://doi.org/10.1007/s00213-013-3369-1>.
- Coddington, L.T., Dudman, J.T., 2019. Learning from action: reconsidering movement signaling in midbrain dopamine neuron activity. *Neuron* 104 (1), 63–77. <https://doi.org/10.1016/j.neuron.2019.08.036>.
- Cook, S.C., Wellman, C.L., 2004. Chronic stress alters dendritic morphology in rat medial prefrontal cortex. *J. Neurobiol.* 60 (2), 236–248. <https://doi.org/10.1002/neu.20025>.
- Dale, A.M., Fischl, B., Sereno, M.I., 1999. Cortical surface-based analysis. I. Segmentation and surface reconstruction. *NeuroImage* 9 (2), 179–194. <https://doi.org/10.1006/nimg.1998.0395>.
- Desikan, R.S., Ségonne, F., Fischl, B., Quinn, B.T., Dickerson, B.C., Blacker, D., Buckner, R.L., Dale, A.M., Maguire, R.P., Hyman, B.T., Albert, M.S., Killiany, R.J., 2006. An automated labeling system for subdividing the human cerebral cortex on MRI scans into gyral based regions of interest. *NeuroImage* 31 (3), 968–980. <https://doi.org/10.1016/j.neuroimage.2006.01.021>.
- Di Salvio, M., Di Giovannantonio, L.G., Omodei, D., Acampora, D., Simeone, A., 2010. Otx2 expression is restricted to dopaminergic neurons of the ventral tegmental area in the adult brain. *Int. J. Dev. Biol.* 54 (5), 939–945. <https://doi.org/10.1387/ijdb.092974ms>.
- Dosenbach, N.U.F., Koller, J.M., Earl, E.A., Miranda-Dominguez, O., Klein, R.L., Van, A.N., Snyder, A.Z., Nagel, B.J., Nigg, J.T., Nguyen, A.L., Wesevich, V., Greene, D.J., Fair, D.A., 2017. Real-time motion analytics during brain MRI improve data quality and reduce costs. *NeuroImage* 161, 80–93. <https://doi.org/10.1016/j.neuroimage.2017.08.025>.
- Douma, E.H., de Kloet, E.R., 2019. Stress-induced plasticity and functioning of ventral tegmental dopamine neurons. *Neurosci. Biobehav. Rev.* 108, 48–77. <https://doi.org/10.1016/j.neubiorev.2019.10.015>.
- Eklund, A., Nichols, T.E., Knutsson, H., 2016. Cluster failure: why fMRI inferences for spatial extent have inflated false-positive rates. *Proc. Natl. Acad. Sci. U.S.A.* 113 (28), 7900–7905. <https://doi.org/10.1073/pnas.1602413113>.
- Evans, G.W., 2004. The environment of childhood poverty. *Am. Psychol.* 59 (2), 77–92. <https://doi.org/10.1037/0003-066X.59.2.77>.
- Fareri, D.S., Gabard-Durnam, L., Goff, B., Flannery, J., Gee, D.G., Lumian, D.S., Caldera, C., Tottenham, N., 2015. Normative development of ventral striatal resting state connectivity in humans. *NeuroImage* 118, 422–437. <https://doi.org/10.1016/j.neuroimage.2015.06.022>.
- Fareri, D.S., Gabard-Durnam, L., Goff, B., Flannery, J., Gee, D.G., Lumian, D.S., Caldera, C., Tottenham, N., 2017. Altered ventral striatal-medial prefrontal cortex resting-state connectivity mediates adolescent social problems after early institutional care. *Dev. Psychopathol.* 29 (5), 1865–1876. <https://doi.org/10.1017/S0954579417001456>.
- Fjell, A.M., Walhovd, K.B., Brown, T.T., Kuperman, J.M., Chung, Y., Hagler Jr, D.J., Venkatraman, V., Roddey, J.C., Erhart, M., McCabe, C., Akshoomoff, N., Amaral, D.G., Bloss, C.S., Libiger, O., Darst, B.F., Schork, N.J., Casey, B.J., Chang, L., Ernst, T.M., et al., 2012. Multimodal imaging of the self-regulating developing brain. *Proc. Natl. Acad. Sci. U.S.A.* 109 (48), 19620–19625. <https://doi.org/10.1073/pnas.1208243109>.
- Gabard-Durnam, L.J., Gee, D.G., Goff, B., Flannery, J., Telzer, E., Humphreys, K.L., Lumian, D.S., Fareri, D.S., Caldera, C., Tottenham, N., 2016. Stimulus-elicited connectivity influences resting-state connectivity years later in human development: a prospective study. *J. Neurosci.* 36 (17), 4771–4784. <https://doi.org/10.1523/JNEUROSCI.0598-16.2016>.
- Gao, W., Alcauter, S., Elton, A., Hernandez-Castillo, C.R., Smith, J.K., Ramirez, J., Lin, W., 2015. Functional Network Development During the First Year: Relative Sequence and Socioeconomic Correlations. *Cereb. Cortex* 25 (9), 2919–2928. <https://doi.org/10.1093/cercor/bhu088>.
- Gomes, F.V., Zhu, X., Grace, A.A., 2019. The pathophysiological impact of stress on the dopamine system is dependent on the state of the critical period of vulnerability. *Mol. Psychiatry*. <https://doi.org/10.1038/s41380-019-0514-1>.
- Gorgolewski, K., Burns, C.D., Madison, C., Clark, D., Halchenko, Y.O., Waskom, M.L., Ghosh, S.S., 2011. Niipyipe: a flexible, lightweight and extensible neuroimaging data processing framework in python. *Front. Neuroinform.* 5, 13. <https://doi.org/10.3389/fninf.2011.00013>.
- Gorgolewski, K.J., Varoquaux, G., Rivera, G., Schwartz, Y., Sochat, V.V., Ghosh, S.S., Maunet, C., Nichols, T.E., Poline, J.-B., Yarkoni, T., Margulies, D.S., Poldrack, R.A., 2016. NeuroVault.org: a repository for sharing unthresholded statistical maps, parcellations, and atlases of the human brain. *NeuroImage* 124 (Pt B), 1242–1244. <https://doi.org/10.1016/j.neuroimage.2015.04.016>.
- Grayson, D.S., Fair, D.A., 2017. Development of large-scale functional networks from birth to adulthood: a guide to the neuroimaging literature. *NeuroImage* 160, 15–31. <https://doi.org/10.1016/j.neuroimage.2017.01.079>.
- Green, J.G., McLaughlin, K.A., Berglund, P.A., Gruber, M.J., Sampson, N.A., Zaslavsky, A.M., Kessler, R.C., 2010. Childhood adversities and adult psychiatric disorders in the national comorbidity survey replication I: associations with first onset of DSM-IV disorders. *Arch. Gen. Psychiatry* 67 (2), 113–123. <https://doi.org/10.1001/archgenpsychiatry.2009.186>.
- Greve, D.N., Fischl, B., 2009. Accurate and robust brain image alignment using boundary-based registration. *NeuroImage* 48 (1), 63–72. <https://doi.org/10.1016/j.neuroimage.2009.06.060>.
- Gruber, M.J., Ranganath, C., 2019. How curiosity enhances hippocampus-dependent memory: the prediction, appraisal, curiosity, and exploration (PACE) framework. *Trends Cogn. Sci.* 23 (12), 1014–1025. <https://doi.org/10.1016/j.tics.2019.10.003>.
- Guerra-Carrillo, B., Mackey, A.P., Bunge, S.A., 2014. Resting-state fMRI: a window into human brain plasticity. *The Neuroscientist: A Review Journal Bringing Neurobiology, Neurology and Psychiatry* 20 (5), 522–533. <https://doi.org/10.1177/1073858414524442>.
- Haber, S.N., Behrens, T.E.J., 2014. The neural network underlying incentive-based learning: implications for interpreting circuit disruptions in psychiatric disorders. *Neuron* 83 (5), 1019–1039. <https://doi.org/10.1016/j.neuron.2014.08.031>.
- Hanson, J.L., Albert, D., Iselin, A.-M.R., Carré, J.M., Dodge, K.A., Hariri, A.R., 2016. Cumulative stress in childhood is associated with blunted reward-related brain activity in adulthood. *Soc. Cogn. Affect. Neurosci.* 11 (3), 405–412. <https://doi.org/10.1093/scan/nsv124>.
- Hanson, J.L., Knott, A.R., Brigidi, B.D., Hariri, A.R., 2017. Heightened connectivity between the ventral striatum and medial prefrontal cortex as a biomarker for stress-related psychopathology: understanding interactive effects of early and more recent stress. *Psychol. Med.* 1–9. <https://doi.org/10.1017/S0033291717003348>.
- Hartley, C.A., Somerville, L.H., 2015. The neuroscience of adolescent decision-making. *Curr. Opin. Behav. Sci.* 5, 108–115. <https://doi.org/10.1016/j.cobeha.2015.09.004>.
- Hauser, T.U., Eldar, E., Dolan, R.J., 2017. Separate mesocortical and mesolimbic pathways encode effort and reward learning signals. *Proc. Natl. Acad. Sci. U.S.A.* 114 (35), E7395–E7404. <https://doi.org/10.1073/pnas.1705643114>.
- Heilbronner, S.R., Hayden, B.Y., 2016. Dorsal anterior cingulate cortex: a bottom-up view. *Annu. Rev. Neurosci.* 39, 149–170. <https://doi.org/10.1146/annurev-neuro-070815-013952>.
- Herzberg, M.P., Gunnar, M.R., 2020. Early life stress and brain function: activity and connectivity associated with processing emotion and reward. *NeuroImage* 209, 116493. <https://doi.org/10.1016/j.neuroimage.2019.116493>.
- Hindly, N.C., Turk-Browne, N.B., 2016. Action-based learning of multistate objects in the medial temporal lobe. *Cereb. Cortex* 26 (5), 1853–1865. <https://doi.org/10.1093/cercor/bhv030>.
- Hollon, N.G., Burgeno, L.M., Phillips, P.E.M., 2015. Stress effects on the neural substrates of motivated behavior. *Nat. Neurosci.* 18 (10), 1405–1412. <https://doi.org/10.1038/nn.4114>.
- Holly, E.N., Miczek, K.A., 2016. Ventral tegmental area dopamine revisited: effects of acute and repeated stress. *Psychopharmacology* 233 (2), 163–186. <https://doi.org/10.1007/s00213-015-4151-3>.
- Hoops, D., Flores, C., 2017. Making dopamine connections in adolescence. *Trends Neurosci.* 40 (12), 709–719. <https://doi.org/10.1016/j.tins.2017.09.004>.
- Hubbard, E.M., Piazza, M., Pinel, P., Dehaene, S., 2005. Interactions between number and space in parietal cortex. *Nat. Rev. Neurosci.* 6 (6), 435–448. <https://doi.org/10.1038/nrn1684>.
- Ironsider, M., Kumar, P., Kang, M.-S., Pizzagalli, D.A., 2018. Brain mechanisms mediating effects of stress on reward sensitivity. *Curr. Opin. Behav. Sci.* 22, 106–113. <https://doi.org/10.1016/j.cobeha.2018.01.016>.
- Jenkinson, M., Beckmann, C.F., Behrens, T.E.J., Woolrich, M.W., Smith, S.M., 2012. FSL. *NeuroImage* 62 (2), 782–790. <https://doi.org/10.1016/j.neuroimage.2011.09.015>.
- Lagraauw, H.M., Kuiper, J., Bot, I., 2015. Acute and chronic psychological stress as risk factors for cardiovascular disease: insights gained from epidemiological, clinical and experimental studies. *Brain Behav. Immun.* 50, 18–30. <https://doi.org/10.1016/j.bbi.2015.08.007>.
- Larsen, B., Olafsson, V., Calabro, F., Laymon, C., Tervo-Clemmens, B., Campbell, E., Minhas, D., Montez, D., Price, J., Luna, B., 2020. Maturation of the human striatal dopamine system revealed by PET and quantitative MRI. *Nat. Commun.* 11 (1), 846. <https://doi.org/10.1038/s41467-020-14693-3>.

- Laureiro-Martinez, D., Brusoni, S., Canessa, N., Zollo, M., 2015. Understanding the exploration-exploitation dilemma: an fMRI study of attention control and decision-making performance. *Strateg. Manage. J.* 36 (3), 319–338. <https://doi.org/10.1002/smj.2221>.
- Lee, H.H.C., Bernard, C., Ye, Z., Acampora, D., Simeone, A., Prochiantz, A., Di Nardo, A. A., Hensch, T.K., 2017. Genetic Otx2 mis-localization delays critical period plasticity across brain regions. *Mol. Psychiatry* 22 (5), 785. <https://doi.org/10.1038/mp.2017.83>.
- Liston, C., Miller, M.M., Goldwater, D.S., Radley, J.J., Rocher, A.B., Hof, P.R., Morrison, J.H., McEwen, B.S., 2006. Stress-induced alterations in prefrontal cortical dendritic morphology predict selective impairments in perceptual attentional set-shifting. *J. Neurosci.* 26 (30), 7870–7874. <https://doi.org/10.1523/JNEUROSCI.1184-06.2006>.
- Lloyd, K., Dayan, P., 2016. Safety out of control: dopamine and defence. *Behav. Brain Funct.* BBF 12 (1), 15. <https://doi.org/10.1186/s12993-016-0099-7>.
- Low, C.A., Salomon, K., Matthews, K.A., 2009. Chronic life stress, cardiovascular reactivity, and subclinical cardiovascular disease in adolescents. *Psychosom. Med.* 71 (9), 927–931. <https://doi.org/10.1097/PSY.0b013e3181ba18ed>.
- Mamiya, P.C., Richards, T., Corrigan, N.M., Kuhl, P.K., 2019. Strength of ventral tegmental area connections with left caudate nucleus is related to conflict monitoring. *Front. Psychol.* 10, 2869. <https://doi.org/10.3389/fpsyg.2019.02869>.
- Marshall, N.A., Marusak, H.A., Sala-Hamrick, K.J., Crespo, L.M., Rabinak, C.A., Thomason, M.E., 2018. Socioeconomic disadvantage and altered corticostriatal circuitry in urban youth. *Hum. Brain Mapp.* 39 (5), 1982–1994. <https://doi.org/10.1002/hbm.23978>.
- Marusak, H.A., Hatfield, J.R.B., Thomason, M.E., Rabinak, C.A., 2017. Reduced Ventral Tegmental Area-Hippocampal Connectivity in Children and Adolescents Exposed to Early Threat. *Biol. Psychiatry Cogn. Neuroimaging* 2 (2), 130–137. <https://doi.org/10.1016/j.bpsc.2016.11.002>.
- McLaughlin, K.A., Sheridan, M.A., 2016. Beyond cumulative risk: a dimensional approach to childhood adversity. *Curr. Dir. Psychol. Sci.* 25 (4), 239–245. <https://doi.org/10.1177/0963721416655883>.
- McLaughlin, K.A., Greif Green, J., Gruber, M.J., Sampson, N.A., Zaslavsky, A.M., Kessler, R.C., 2012. Childhood adversities and first onset of psychiatric disorders in a national sample of US adolescents. *Arch. Gen. Psychiatry* 69 (11), 1151–1160. <https://doi.org/10.1001/archgenpsychiatry.2011.2277>.
- Merrick, M.T., Ford, D.C., Ports, K.A., Guinn, A.S., 2018. Prevalence of adverse childhood experiences from the 2011–2014 behavioral risk factor surveillance system in 23 states. *JAMA Pediatr.* 172 (11), 1038–1044. <https://doi.org/10.1001/jamapediatrics.2018.2537>.
- Mitra, A., Snyder, A.Z., Blazey, T., Raichle, M.E., 2015. Lag threads organize the brain's intrinsic activity. *Proc. Natl. Acad. Sci. U.S.A.* 112 (17), E2235–E2244. <https://doi.org/10.1073/pnas.1503960112>.
- Monnat, S.M., Chandler, R.F., 2015. Long term physical health consequences of adverse childhood experiences. *Sociol. Q.* 56 (4), 723–752. <https://doi.org/10.1111/tsq.12107>.
- Murphy, K., Birn, R.M., Bandettini, P.A., 2013. Resting-state fMRI confounds and cleanup. *NeuroImage* 80, 349–359. <https://doi.org/10.1016/j.neuroimage.2013.04.001>.
- Murphy, A., Steele, H., Steele, M., Allman, B., Kastner, T., Dube, S.R., 2016. The clinical adverse childhood experiences (ACES) questionnaire: implications for trauma-informed behavioral healthcare. In: Briggs, R.D. (Ed.), *Integrated Early Childhood Behavioral Health in Primary Care: A Guide to Implementation and Evaluation*, Vol. 212, pp. 7–16. [https://doi.org/10.1007/978-3-319-31815-8\\_2](https://doi.org/10.1007/978-3-319-31815-8_2).
- Murty, V.P., Shermohammed, M., Smith, D.V., Carter, R.M., Huettel, S.A., Adcock, R.A., 2014. Resting state networks distinguish human ventral tegmental area from substantia nigra. *NeuroImage* 100, 580–589. <https://doi.org/10.1016/j.jneuroimage.2014.06.047>.
- Murty, V.P., Calabro, F., Luna, B., 2016. The role of experience in adolescent cognitive development: integration of executive, memory, and mesolimbic systems. *Neurosci. Biobehav. Rev.* 70, 46–58. <https://doi.org/10.1016/j.neubiorev.2016.07.034>.
- Murty, V.P., Shah, H., Montez, D., Foran, W., Calabro, F., Luna, B., 2018. Age-related trajectories of functional coupling between the VTA and nucleus accumbens depend on motivational state. *J. Neurosci.* 38 (34), 7420–7427. <https://doi.org/10.1523/JNEUROSCI.3508-17.2018>.
- Novick, A.M., Levandowski, M.L., Laumann, L.E., Philip, N.S., Price, L.H., Tyrka, A.R., 2018. The effects of early life stress on reward processing. *J. Psychiatr. Res.* 101, 80–103. <https://doi.org/10.1016/j.jpsychires.2018.02.002>.
- Omodei, D., Acampora, D., Mancuso, P., Prakash, N., Di Giovannantonio, L.G., Wurst, W., Simeone, A., 2008. Anterior-posterior graded response to Otx2 controls proliferation and differentiation of dopaminergic progenitors in the ventral mesencephalon. *Development* 135 (20), 3459–3470. <https://doi.org/10.1242/dev.027003>.
- Operario, D., Adler, N.E., Williams, D.R., 2004. Subjective social status: reliability and predictive utility for global health. *Psychol. Health* 19 (2), 237–246. <https://doi.org/10.1080/08870440310001638098>.
- Palacios-Barrios, E.E., Hanson, J.L., 2019. Poverty and self-regulation: connecting psychosocial processes, neurobiology, and the risk for psychopathology. *Compr. Psychiatry* 90, 52–64. <https://doi.org/10.1016/j.comppsych.2018.12.012>.
- Palomero-Gallagher, N., Amunts, K., Zilles, K., 2015. Transmitter receptor distribution in the human brain. In: Toga, A.W. (Ed.), *Brain Mapping*. Academic Press, pp. 261–275. <https://doi.org/10.1016/B978-0-12-397025-1.00221-9>.
- Peña, C.J., Kronman, H.G., Walker, D.M., Cates, H.M., Bagot, R.C., Purushothaman, I., Issler, O., Loh, Y.-H.E., Leong, T., Kiraly, D.D., Goodman, E., Neve, R.L., Shen, L., Nestler, E.J., 2017. Early life stress confers lifelong stress susceptibility in mice via ventral tegmental area OTX2. *Science* 356 (6343), 1185–1188. <https://doi.org/10.1126/science.aan4491>.
- Poldrack, R.A., 2017. Precision neuroscience: dense sampling of individual brains. *Neuron* 95 (4), 727–729. <https://doi.org/10.1016/j.neuron.2017.08.002>.
- Preibisch, C., Castrillón, G., J. G., Bührer, M., Riedl, V., 2015. Evaluation of multiband EPI acquisitions for resting state fMRI. *PLoS One* 10 (9), e0136961. <https://doi.org/10.1371/journal.pone.0136961>.
- Reynolds, L.M., Pokinko, M., Torres-Berrío, A., Cuesta, S., Lambert, L.C., Del Cid Pellitero, E., Wodzinski, M., Manitt, C., Krimpenfort, P., Kolb, B., Flores, C., 2018. DCC receptors drive prefrontal cortex maturation by determining dopamine axon targeting in adolescence. *Biol. Psychiatry* 83 (2), 181–192. <https://doi.org/10.1016/j.biopsych.2017.06.009>.
- Richter, A., Krämer, B., Diekhof, E.K., Gruber, O., 2019. Resilience to adversity is associated with increased activity and connectivity in the VTA and hippocampus. *NeuroImage Clin.* 23, 101920. <https://doi.org/10.1016/j.nicl.2019.101920>.
- Roche, A., 2011. A four-dimensional registration algorithm with application to joint correction of motion and slice timing in fMRI. *IEEE Trans. Med. Imaging* 30 (8), 1546–1554. <https://doi.org/10.1109/TMI.2011.2131152>.
- Russo, S.J., Nestler, E.J., 2013. The brain reward circuitry in mood disorders. *Nat. Rev. Neurosci.* 14 (9), 609–625. <https://doi.org/10.1038/nrn3381>.
- Salamone, J.D., Correa, M., 2012. The mysterious motivational functions of mesolimbic dopamine. *Neuron* 76 (3), 470–485. <https://doi.org/10.1016/j.neuron.2012.10.021>.
- Salehi, M., Greene, A.S., Karbasi, A., Shen, X., Scheinost, D., Constable, R.T., 2020. There is no single functional atlas even for a single individual: functional parcel definitions change with task. *NeuroImage* 208, 116366. <https://doi.org/10.1016/j.neuroimage.2019.116366>.
- Shmueli, K., van Gelderen, P., de Zwart, J.A., Horovitz, S.G., Fukunaga, M., Jansma, J. M., Duyu, J.H., 2007. Low-frequency fluctuations in the cardiac rate as a source of variance in the resting-state fMRI BOLD signal. *NeuroImage* 38 (2), 306–320. <https://doi.org/10.1016/j.neuroimage.2007.07.037>.
- Smith, S.M., 2002. Fast robust automated brain extraction. *Hum. Brain Mapp.* 17 (3), 143–155. <https://doi.org/10.1002/hbm.10062>.
- Somerville, L.H., Casey, B.J., 2010. Developmental neurobiology of cognitive control and motivational systems. *Curr. Opin. Neurobiol.* 20 (2), 236–241. <https://doi.org/10.1016/j.conb.2010.01.006>.
- Somerville, L.H., Jones, R.M., Casey, B.J., 2010. A time of change: behavioral and neural correlates of adolescent sensitivity to appetitive and aversive environmental cues. *Brain Cogn.* 72 (1), 124–133. <https://doi.org/10.1016/j.bandc.2009.07.003>.
- Sugama, S., Kakinuma, Y., 2016. Loss of dopaminergic neurons occurs in the ventral tegmental area and hypothalamus of rats following chronic stress: possible pathogenetic loci for depression involved in Parkinson's disease. *Neurosci. Res.* 111, 48–55. <https://doi.org/10.1016/j.neures.2016.04.008>.
- Tak, S., Polimeni, J.R., Wang, D.J.J., Yan, L., Chen, J.J., 2015. Associations of resting-state fMRI functional connectivity with flow-BOLD coupling and regional vasculature. *Brain Connect.* 5 (3), 137–146. <https://doi.org/10.1089/brain.2014.0299>.
- Tisdall, M.D., Hess, A.T., Reuter, M., Meintjes, E.M., Fischl, B., van der Kouwe, A.J.W., 2012. Volumetric navigators for prospective motion correction and selective reacquisition in neuroanatomical MRI. *Magn. Reson. Med.* 68 (2), 389–399. <https://doi.org/10.1002/mrm.23228>.
- Tomasi, D., Volkow, N.D., 2014. Functional connectivity of substantia nigra and ventral tegmental area: maturation during adolescence and effects of ADHD. *Cereb. Cortex* 24 (4), 935–944. <https://doi.org/10.1093/cercor/cbs382>.
- Watabe-Uchida, M., Zhu, L., Ogawa, S.K., Vamanrao, A., Uchida, N., 2012. Whole-brain mapping of direct inputs to midbrain dopamine neurons. *Neuron* 74 (5), 858–873. <https://doi.org/10.1016/j.neuron.2012.03.017>.
- Westbrook, A., van den Bosch, R., Määttä, J.I., Hofmans, L., Papadopetraki, D., Cools, R., Frank, M.J., 2020. Dopamine promotes cognitive effort by biasing the benefits versus costs of cognitive work. *Science* 367 (6484), 1362–1366. <https://doi.org/10.1126/science.aaaz5891>.
- Yamaguchi, T., Wang, H.-L., Li, X., Ng, T.H., Morales, M., 2011. Mesocorticolimbic glutamatergic pathway. *The Journal of Neuroscience: The Official Journal of the Society for Neuroscience* 31 (23), 8476–8490. <https://doi.org/10.1523/JNEUROSCI.1598-11.2011>.
- Yeo, B.T.T., Krienen, F.M., Sepulcre, J., Sabuncu, M.R., Lashkari, D., Hollinshead, M., Roffman, J.L., Smoller, J.W., Zöllei, L., Polimeni, J.R., Fischl, B., Liu, H., Buckner, R. L., 2011. The organization of the human cerebral cortex estimated by intrinsic functional connectivity. *J. Neurophysiol.* 106 (3), 1125–1165. <https://doi.org/10.1152/jn.00338.2011>.
- Zisner, A., Beauchaine, T.P., 2015. Midbrain neural mechanisms of trait impulsivity. *Oxford Handbook of Externalizing Spectrum Disorders*, pp. 184–200. <https://books.google.com/books?hl=en&lr=&id=f5yOCgAAQBAJ&oi=fnd&pg=PA184&dq=mesocorticolimbic+impulsive+behavior+children&ots=QKb49Qww9P&sig=qfhhEYgFXEb9FdWdSUTeB1TSfo>.